ARCHIVES OF ACOUSTICS
Vol. **45**, No. 2, pp. 359–365 (2020)
DOI: 10.24425/aoa.2020.133156

Technical Note

Experimental Study on the Half Flat Tip Serrated Trailing Edge for Stand Fan

Hsiao Mun LEE[(1,2)], Kian Meng LIM[(2)], Jinlong XIE[(3)*], Heow Pueh LEE[(2)]

[(1)] *Center for Research on Leading Technology of Special Equipment*
School of Mechanical and Electric Engineering, Guangzhou University
230 Wai Huan Xi Road, Guangzhou 510006, P.R.China; e-mail: hmlee@gzhu.edu.cn

[(2)] *Department of Mechanical Engineering, National University of Singapore*
9 Engineering Drive 1, Singapore 117575, Singapore; e-mail: {limkm, mpeleehp}nus.edu.sg

[(3)] *School of Mechanical and Electric Engineering, Guangzhou University*
230 Wai Huan Xi Road, Guangzhou 510006, P.R.China
*Corresponding Author e-mail: jlxie@gzhu.edu.cn

(*received October 19, 2018; accepted January 15, 2020*)

The effectiveness of half flat tip serrations on reducing fan blade trailing edge noise was investigated using experimental methods. The experiments were conducted at an anechoic chamber under different rotating fan speeds. Numerical simulations were performed to investigate the mass flow rate generated by the serrated fan and compared with that by the baseline fan. The experimental results showed that the overall amount of noise reduction decreased with the increasing of the distance away from the fan. It was found that the effectiveness of the serrations was not proportional with the rotating speed of the fan where it was most effective at 263 rpm and 2041 rpm with noise reductions about 3.1 dBA and 3.5 dBA, respectively. This phenomenon might be depended on how trailing edge vortex would interact with the serrations at different speeds of the fan. The reduction of mass flow rate reduced with the increasing of the rotating speed and the highest reduction was found at 263 rpm which was about 18% and this reduction was accompanied by overall noise reduction of 3.1 dBA.

Keywords: trailing edge noise; half flat tip; serration; stand fan.
Subject classification code: T210 (CERIF).

List of notations

- h – serration amplitude [m],
- L_{Aeq} – equivalent sound pressure level [dBA],
- ΔL_{Aeq} – reduction of equivalent sound pressure level [dBA],
- ΔQ – reduction of mass flow rate [%],
- Q_o – mass flow rate of baseline fan [kg/s],
- Q_s – mass flow rate of serrated fan [kg/s],
- R – blade radius [m],
- Re_c – Reynolds number,
- λ – serration spanwise length [m].

1. Introduction

Aerodynamic noises on rotating machinery such as noises generated from pump, turbine and fan are ongoing issue for the past three decades. Aerodynamic noise sources on rotating machinery can be divided into two main categories (Barone, 2011). The first category is the turbulent inflow noise due to scattering of turbulent wind fluctuations by the blades of rotating machinery. The second category is the airfoil self-noise due to interaction of a nominally steady flow with the blades of rotating machinery. Airfoil self-noise can be further divided into two noise mechanisms where they are blade tip vortex noise and trailing edge noise. Oerlemans *et al.* (2007) and Oerlemans and Schepers (2009) measured blade noise for a 850 kW Gamesa G58 wind turbine and a 2.3 MW GE wind turbine, respectively. They found that blade noise was not loudest at the blade tip and this indicated that tip vortex noise was not the dominant airfoil self-noise. Therefore, the scope of current studies will be focused on trailing edge noise of rotating machinery where one of the noise reduction technique which is serrated trailing edge will be investigated.

Howe (1991) studied the production of sound by low Mach number turbulent flow over the trailing edge of a serrated airfoil. He concluded that at high frequencies, the predicted attenuation was about 1 dB and 7 or 8 dB when $\lambda/h \asymp 10$ and $\lambda/h = 1$, respectively. λ and h were the serrations spanwise length and amplitude, respectively. The effects of serrated trailing edge on the flow field downstream of an idealized aircraft blade were investigated by Geiger (2004) through measurement in a low speed cascade tunnel. They found that the mean streamwise velocity and turbulent kinetic energy in the blade tip region were nearly the same for serrated as well as the baseline blades. Arce-Leon (2010) analyzed the effects of serrations fitted on a section of a wind turbine blade on noise generation using numerical method. He concluded that noise could be mitigated by using serrated trailing edge because it extended the ranges of turbulence length scales. Therefore, it reduced the effect of constructive interference from pressure fluctuations generated by eddies shed from the trailing edge of the blade. Liang *et al.* (2010) designed few biological sawtooth-shaped edges and applied them on the trailing edge of a impeller fan vane. They found that the sawtooth-shaped edges were good for preventing formation of off-body vortex, improved the turbulence intensity of trailing edge flow and hence, reduced noise generation. Moreau and Doolan (2013) explored the noise-reduction potential of sawtooth trailing edge serrations on a flat plate from low to moderate Reynolds number ($1.6{\cdot}10^5 < \mathrm{Re}_c < 4.2{\cdot}10^5$) through experimental investigation. They concluded that trailing edge serrations were able to achieve noise reduction of 13 dB in the narrowband noise levels due to the reduction of vortex shedding at the trailing edge. Nies *et al.* (2015) investigated the flow around a generic airfoil with blunt and serrated trailing edges in compressible subsonic and transonic conditions by experimental method. They found that for free stream Mach number up to 0.79, the serrations significantly reduced the pressure wave amplitude and the amount of reduction was proportional to the serration length.

Chong and Vathylakis (2015a) studied the phenomenon of turbulent flow over a flat plate with serrated sawtooth trailing edge. They found that the interaction between the local turbulent boundary layer and the vortical structures resulted in a redistribution of the turbulent shear stress and momentum transport near the sawtooth side and tip and thus, affected the self noise radiation. Chong and Vathylakis (2015b) developed a poro-serrated concept where they used porous metal, thin brush bundles or synthetic foam to fill the gaps between adjacent members of the sawtooth on the nonflat plate trailing edge. They found 7 dB of broadband noise reduction for the nonflat plate without compromising the aerodynamic performances in lift and drag by using the poro-serrated concept. Chong and Dubois (2016) reported an aeroacoustic investigation of a NACA0012 airfoil with different poro-serrated trailing edge configurations where it contained porous materials with different flow resistivity. Their results showed that with the optimal choice of the porous material, the airfoil with poro-serrated trailing edge could achieve additional 1.5 dB of noise reduction in the broadband noise compared to conventional serrated trailing edge.

The three-dimensional flow field over the suction side of a NACA 0018 airfoil with trailing edge serrations was studied by Avallone *et al.* (2016) using time-resolved tomographic particle image velocimetry. They found that the boundary layer thickness decreased along the streamwise direction with a corresponding reduction of the size of the turbulent structures developing over the suction side of the serrations. The broadband noise generated by the scattering of turbulent flow at the trailing edge of a NACA 0018 airfoil with trailing edge serrations was investigated by Arce-Leon *et al.* (2017) by varying both the airfoil angle of attack and serration flap angle. They claimed that the noise level generated by the serrated airfoil was higher than that of the airfoil without serrations at frequencies beyond a crossover value. The wake distribution of a serrated airfoil was studied by Ryi and Choi (2017) through wind tunnel testing. Avallone *et al.* (2018) investigated the far-field noise and the hydrodynamic flow field of a conventional sawtooth and a combed-sawtooth airfoils through solving lattice Boltzmann equation. They confirmed that the combed-sawtooth serrations reduced noise more than the conventional sawtooth serrations at low and mid frequency range. Jaron *et al.* (2018) implemented serrations at the front-rotor of a contra-rotating open rotor in order to increase the wake mixing and thus reduce the tones through Reynolds-averaged Navier-Stokes simulation. Their results confirmed that tonal interaction noise could be reduced by means of trailing edge serrations. Six ceiling fan blade models with different types of trailing edge serrations were studied by Lee *et al.* (2018) used numerical method in order to investigate the effectiveness of serrations in reducing fan blade trailing edge noise. Their simulation results showed that the half flat tip fan blade had the best acoustical performance where it could obtain an overall noise reduction of 13.9 dBA.

It can be seen that the reported studies on serrated trailing edge were mostly confined to industry machines such as wind turbine and aircraft airfoil while only limited study was conducted for the case of home appliance machine such as stand fan. Stand fan is a common machine wisely used in home or office due to its high movability and low cost. However, standing fan produces annoying noise especially when it rotates at high speed. Therefore, the main objective of the current effort is to use experimental method to investigate the effectiveness of half flat tip serrations on reducing fan blade trailing edge noise. Numerical simulations were performed in this study to investigate the mass flow rate generated by the serrated fan and compared with that of conventional fan.

2. Experimental methods

The stand fan under investigation was a household stand fan with blade radius R of about 0.2 m and rotated in clockwise direction. The baseline fan consisted of three metal blades which made of aluminum and zinc as shown in Fig. 1a. For the modified fan, conventional serrated edges were modified to half flat tip serrated edges as shown in Fig. 1b where the serrations only started from $0.6R$ of the blades and the sharp tips of the serrations were also modified to flat tips. The purpose of such modification is to reduce the cut-off area due to the serrations and hence, improves the mass flow rate that generated by the fan. In addition, flat tips are also safer than sharp tips because user of the fan can easily wounded by the sharp tips when the user is conducting cleaning or other jobs on the fan. It should be noted that flat tips are not completely safe if the blades are rotating at high speed, so all measurements in the present studies were conducted with special care. λ and h of the serrations in the present study were 7.87 mm and 7.26 mm, respectively, and therefore, $\lambda/h \approx 1$. According to the prediction from Howe (1991), the estimated noise attenuation should be around 7 or 8 dB at high frequencies.

a) b)

Fig. 1. Stand fan with: a) baseline blades, b) half flat tip serrated blades.

All measurements were conducted at an anechoic chamber. The blades and hub of the fan were mounted on a table and were connected to a motor as shown in Fig. 2. Rotation speeds of the fan were controlled using the motor equipped with a speed controller so that the rotating speeds of the baseline and the serrated fans were similar. Three Class 1 sound level meters were placed at 0.5 m or 1 m in front of the fan. The first meter was located at the central of the fan. The second and third meters were located at 0.3 m ($1.5R$) and 0.5 m ($2.5R$) away from the central of the fan, respectively. All data were recorded using the sound level meters from 25 Hz to 4000 Hz. The experiments were

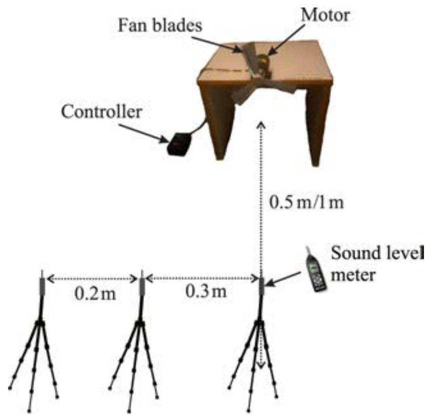

Fig. 2. Experimental set-up.

conducted under four rotating speeds: 263, 1060, 2041, and 3285 rpm. The insertion loss (IL) was obtained by:

$$\text{IL} = \text{SPL}_{\text{baseline fan}} - \text{SPL}_{\text{serrated fan}}, \tag{1}$$

where SPL is the sound pressure level. Equivalent SPL (L_{Aeq}) was calculated for each set of data by taking into account contribution of noise from each frequency which is given by:

$$L_{\text{Aeq}} = 10 \log \sum_{i=1}^{n} t_i 10^{\left(\frac{\text{SPL}_i}{10}\right)}, \tag{2}$$

where i and n represent the first and last SPLs in the measured frequency range, respectively and t_i is the fraction of the time period that the noise has a sound level of SPL_i. After that, reduction of L_{Aeq} (ΔL_{Aeq}) is obtained by:

$$\Delta L_{\text{Aeq}} = L_{\text{Aeq (baseline fan)}} - L_{\text{Aeq (serrated fan)}}. \tag{3}$$

2.1. Uncertainty analysis

The uncertainty of an experiment is caused by random and systematic errors. Random error can be treated statistically in the experiment while systematic error can be minimised by careful experimental methods. Systematic error of the current noise measurement is mostly depends on the locations of the sound level meters and the stand fan where they need to be placed at the same location for all experiments. The locations of the sound level meters and the stand fan were labelled so that these equipment can be placed at the same location for all experiments in order to minimise the systematic error. The random error σ of the current noise measurement is given as:

$$\sigma = \sqrt{(\Delta x)^2 + \ldots + (\Delta z)^2}, \tag{4}$$

where x and z are all the parameters used in all equations in the particular study. For Eqs (1)–(3) in the present study, SPL is the only parameter contributes to those equations. Therefore, $\sigma = \Delta\mathrm{SPL} \approx \pm 1.43\%$ where it is computed by 1 dBA/70 dBA as Class 1 sound level meter typically has an accuracy of ± 1 dBA and the maximum SPL in the current noise measurement is about 70 dBA.

3. Numerical methods

From literature reviews, it is clear that the aerodynamic performance of an airfoil was degraded with implementation of serrated trailing edge due to reduction of effective surface area of the airfoil. Similar to the case of airfoil, the mass flow rate that generated by the serrated fan was definitely lower than that of baseline fan due to reduction of the effective surface area of the serrated fan blade. Therefore in the present studies, beside the acoustical performance of the serrated fan, the effects of serrations on the mass flow rate that generated by the fan were also examined. The mass flow rate that generated by the fan cannot be measured using flow meter because the flow was not uniform and it was highly turbulent. Consequently, the variation of the mass flow rate was extremely high within the measurement area. Since it is not realistic to place few hundreds flow meters to measure the overall mass flow rate within the measurement area, numerical simulations were performed on the fan using ANSYS (Fluent) software in order to capture the overall mass flow rate that generated by the fan. In the numerical model, the mass flow rate over a plane with radius of 0.4 m and located at 0.5 m in front of the fan was computed. The simulations were also conducted under four rotating speeds: 263, 1060, 2041, and 3285 rpm. The computational domain was extended $6R$ in length from inlet to the fan and also $8R$ from the fan to outlet along z direction as shown in Fig. 3. For radial direction, the computational domain was extended about $4R$ in length. Constant atmosphere pressure distributions were applied at both inlet and outlet. Smooth surface was applied on the fan blades and hub with no slip wall boundary configuration. Wall boundary condition was also applied on the outer cylinder surface

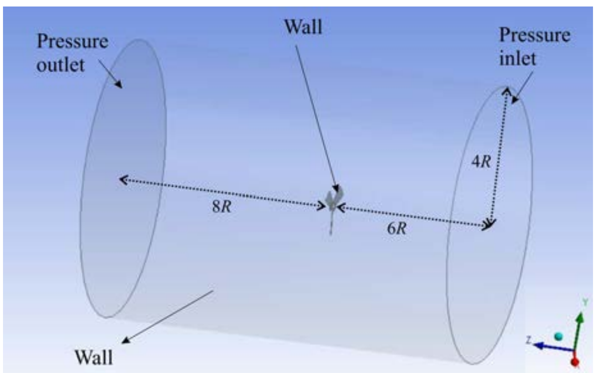

Fig. 3. Computational domain and boundary conditions of the numerical model.

as $4R$ of length in radial direction was long enough to assume there is no change of flow pattern in the farfield atmospheric environment. A tetrahedron grid was generated and there were 7.9 million cells in the computational domain. The average element quality is about 0.83. The $k\omega$-SST turbulence model was used in the simulation. The reduction of mass flow rate [%] is defined as:

$$\Delta Q = \frac{Q_o - Q_s}{Q_o} \cdot 100\%, \tag{5}$$

where Q_o and Q_s are the mass flow rates generated by the baseline and serrated fans, respectively.

4. Results and discussion

Figure 4 shows the IL obtained by the serrated fan at 0.5 m under different rotating speeds. The results for

a)

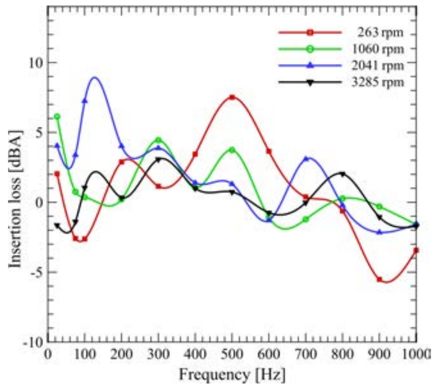

b)

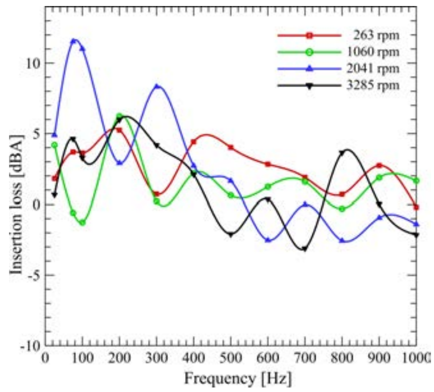

c)

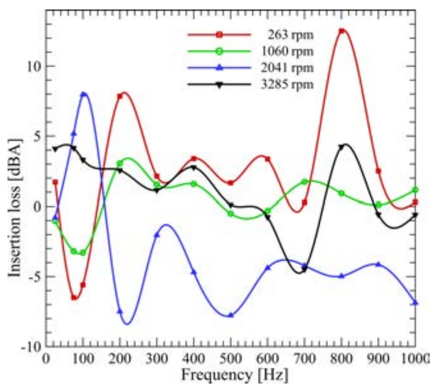

Fig. 4. Insertion loss obtained by the serrated fan at 0.5 m under different rotating speeds: a) central, b) $1.5R$, c) $2.5R$.

the frequencies above 1000 Hz are not presented in this paper because the serrations do not help in reducing the trailing edge noise for frequencies above 1000 Hz. This observation opposes with the conclusion from Chong and Vathylakis (2015b) where they claimed that the serrated trailing edge could obtain noise attenuation at high frequencies. It can be observed from Fig. 4a that the serrated fan produces similar trends of IL for all rotating speeds at the central of the fan. Generally, the amount of IL obtained decreases gradually with the increasing of the frequency. Two obvious peaks of IL are found at 100 Hz and 500 Hz when the rotating speeds are equal to 2041 rpm and 263 rpm, respectively. Therefore, ΔL_{Aeq} as high as 4.2 dBA and 4.1 dBA are obtained for these two rotating speeds as shown in Table 1, respectively. The overall values shown in Tables 1 and 2 are obtained by averaging the ΔL_{Aeq} from all measurement locations (central, $1.5R$ and $2.5R$) for each rotating speed. The results at $1.5R$ are similar to that of the central of the fan where the serrated fan also produces similar trends of IL for all rotating speeds. Highest ΔL_{Aeq} is also found at 2041 rpm which is about 5.7 dBA and then followed by 263 rpm which is about 2.9 dBA (see Table 1). The results at $2.5R$ are different with the other two positions where the serrated fan obtains negative IL at 2041 rpm for frequencies above 100 Hz (see Fig. 4c). For the other three rotating speeds at $2.5R$, the amount of IL obtained also decreases gradually with the increasing of the frequency except at 800 Hz where the peaks of IL are found for 263 rpm and 3285 rpm at this frequency. It can be concluded from Table 1 that the serrations produce highest overall ΔL_{Aeq} at 2041 rpm and then followed by 263 rpm.

Table 1. ΔL_{Aeq} obtained by the serrated fan at 0.5 m. All units are in dBA.

Position/Rotating speed [rpm]	263	1060	2041	3285
Central	4.1	1.8	4.2	0.5
$1.5R$	2.9	1.2	5.7	1.3
$2.5R$	2.1	0.6	−0.6	1.0
Overall	3.1	1.2	3.5	0.9

Table 2. ΔL_{Aeq} obtained by the serrated fan at 1 m. All units are in dBA.

Position/Rotating speed [rpm]	263	1060	2041	3285
Central	1.5	1.0	−0.6	−1.1
$1.5R$	3.2	1.4	3.7	2.7
$2.5R$	1.3	1.3	2.3	0.1
Overall	2.0	1.3	2.0	0.7

Figure 5 shows the IL obtained by the serrated fan at 1 m under different rotating speeds. The trends of the IL at central of the fan for all rotating speeds are slightly different with that at 0.5 m (see Fig. 4a) where

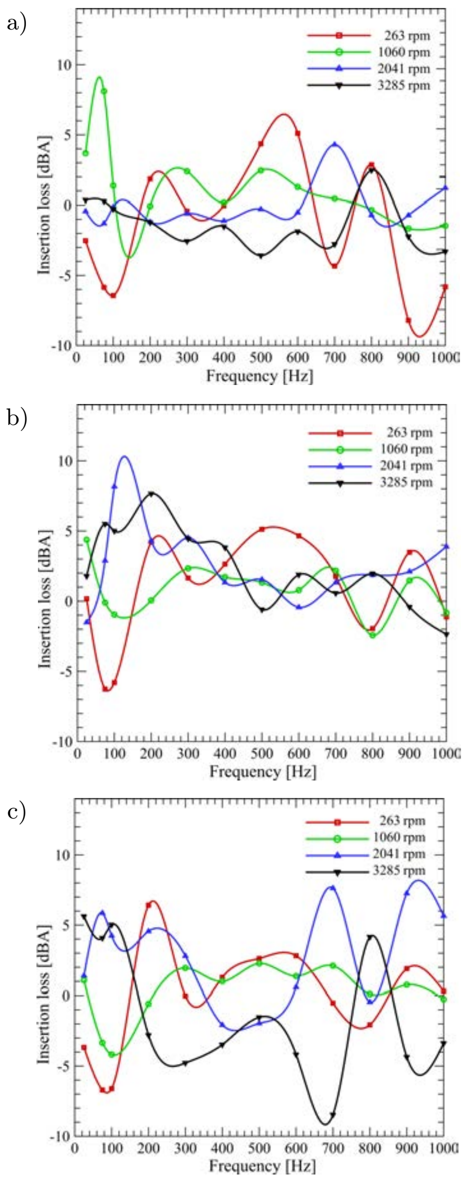

Fig. 5. Insertion loss obtained by the serrated fan at 1 m under different rotating speeds: a) central, b) $1.5R$, c) $2.5R$.

at 1 m, the IL no longer decreases gradually with the increasing of frequency. Two obvious peaks of IL are found at 75 Hz and 600 Hz when the rotating speeds are equal to 1060 rpm and 263 rpm, respectively. It can be observed from Table 2 that the ΔL_{Aeq} obtained by the serrated fan decreases at 1 m at central of the fan for all rotating speeds compared to that at 0.5 m (see Table 1). At $1.5R$, the ΔL_{Aeq} obtained by the serrated fan for all rotating speeds are higher than that at the central of the fan. Similar to the IL at 0.5 m, the variations of the IL among different rotating speeds at $2.5R$ are also larger than that at central and $1.5R$. In addition, serrated fan obtains negative IL at 3285 rpm for frequencies above 100 Hz except at 800 Hz. At 1 m, it also can be concluded from Table 2 that the serrations produce highest overall ΔL_{Aeq} at 263 rpm and

2041 rpm. However, the amounts of noise reduction are lower at 1 m for these two rotating speeds compared to that at 0.5 m. Table 3 shows the mass flow rate reduction of the serrated fan under different rotating speeds. It is found that the reduction of mass flow rate reduces with the increasing of the rotating speed and the highest reduction is found at 263 rpm which is about 18%.

Table 3. ΔQ under different rotating speeds.

Rotating speed [rpm]	263	1060	2041	3285
ΔQ [%]	18	13	9	7

5. Conclusions

The effectiveness of half flat tip serrations on reducing fan blade trailing edge noise was investigated using experimental methods. The experiments were conducted at an anechoic chamber under different rotating fan speeds. The noise data were collected at three different locations (central, $1.5R$, and $2.5R$) in front of the fan. These three sets of measurements were conducted twice at 0.5 m and 1 m away from the fan. Numerical simulations were performed to investigate the mass flow rate generated by the serrated fan and compared with that by the baseline fan. The serrated fan in the present studies had the blade geometry of $\lambda/h \approx 1$ where the estimated noise attenuation should be around 7 or 8 dB at high frequencies according to Howe (1991). However, our experimental results showed that the half flat tip serrations did not help in reducing the fan trailing edge noise for frequencies above 1000 Hz. Generally, at 0.5 m away from the fan, the amount of noise reduction decreased with the increasing of frequency at central and $1.5R$. However, this phenomenon could not be observed at 1 m away from the fan. At $2.5R$, the variations of the amount of noise reduction among different rotating speeds were larger than the other two positions. The overall amount of noise reduction decreased with the increasing of the distance away from the fan. It was found that the effectiveness of the serrations was not proportional with the rotating speed of the fan where it was most effective at 263 rpm and 2041 rpm with noise reductions about 3.1 dBA and 3.5 dBA, respectively. This phenomenon might be depended on how trailing edge vortex would interact with the serrations at different speeds of the fan. Further studies included flow visualization on the blade trailing edge is needed in order to clarify the mechanism of how rotating speed of the fan would affect the noise reduction performance of serrations. Finally, from the results of the numerical simulations, it was found that the reduction of mass flow rate reduced with the increasing of the rotating speed. The highest reduction was found at 263 rpm which was about 18% and this reduction was accompanied by overall noise reduction of 3.1 dBA.

Acknowledgements

This research was funded by Singapore Ministry of National Development and National Research Foundation [L2NICCFP1-2013-8], National Natural Science Foundation of China [51908142] and Natural Science Foundation of Guangdong Province [2019A1515012223, 2018A030313878].

References

1. Arce-Leon C.A. (2010), *Modelling of serrated trailing edges to reduce aerodynamic noise in wind turbine*, PhD thesis, Uppsala Universitet, Sweden.
2. Arce-Leon C. *et al.* (2017), Effect of trailing edge serration-flow misalignment on airfoil noise emissions, *Journal of Sound and Vibration*, **405**: 19–33, doi: 10.1016/j.jsv.2017.05.035.
3. Avallone F., Probsting S., Ragni D. (2016), Three-dimensional flow field over a trailing-edge serration and implications on broadband noise, *Physics of Fluids*, **28**(11): 117101 (20 pp.), doi: 10.1063/1.4966633.
4. Avallone F., Van Der Velden W.C.P., Ragni D., Casalino D. (2018), Noise reduction mechanisms of sawtooth and combed-sawtooth trailing-edge serrations, *Journal of Fluid Mechanics*, **848**: 560–591, doi: 10.1017/jfm.2018.377.
5. Barone M.F. (2011), *Survey of techniques for reduction of wind turbine blade trailing edge noise*, Sandia National Laboratories.
6. Chong T.P., Dubois E. (2016), Optimization of the poro-serrated trailing edges for airfoil broadband noise reduction, *The Journal of the Acoustical Society of America*, **140**(2): 1361–1373, doi: 10.1121/1.4961362.
7. Chong T.P., Vathylakis A. (2015a), On the aeroacoustic and flow structures developed on a flat plate with a serrated sawtooth trailing edge, *Journal of Sound and Vibration*, **354**: 65–90, doi: 10.1016/j.jsv.2015.05.019.
8. Chong T.P., Vathylakis A. (2015b), Poro-serrated trailing-edge devices for airfoil self-noise reduction, *AIAA Journal*, **53**(11): 3379–3394, doi: 10.2514/1.J053983.
9. Geiger D.H. (2004), *Comparative analysis of serrated trailing edge designs on idealized aircraft engine fan blades for noise reduction*, Virginia Polytechnic Institute and State University.
10. Howe M.S. (1991), Aerodynamic noise of a serrated trailing edge, *Journal of Fluids and Structures*, **5**(1): 33–45, doi: 10.1016/0889-9746(91)80010-B.
11. Jaron R., Moreau A., Guerin S., Schnell R. (2018), Optimization of trailing-edge serrations to reduce open-rotor tonal interaction noise, *Journal of Fluids Engineering*, **140**(2): 021201 (12 pp.), doi: 10.1115/1.4037981.

12. Lee H.M., Lim K.M., Lee H.P. (2018), Reduction of ceiling fan noise by serrated trailing edge, *Fluctuation and Noise Letters*, **17**(3): 1850026 (11 pp.), doi: 10.1142/S0219477518500268.

13. Liang G.Q., Wang J.C., Chen Y., Zhou C.H., Liang J., Ren L.Q. (2010), The study of owl's silent flight and noise reduction on fan vane with bionic structure, *Advances in Natural Science*, **3**(2): 192–198, doi: 10.3968/j.ans.1715787020100302.022.

14. Moreau D.J., Doolan C.J. (2013), Noise-reduction mechanism of a flat-plate serrated trailing edge, *AIAA Journal*, **51**(10): 2513–2522, doi: 10.2514/1.J052436.

15. Nies J.M., Gageik M.A., Klioutchnikov I., Olivier H. (2015), Investigation of wave phenomena on a blunt airfoil with straight and serrated trailing edges, *Experiments in Fluids,* **56**(7): 136 (14 pp.), doi: 10.1007/s00348-015-2009-4.

16. Oerlemans S., Schepers J.G. (2009), Prediction of wind turbine noise and validation against experiment, *International Journal of Aeroacoustics*, **8**(6): 555–884, doi: 10.1260/147547209789141489.

17. Oerlemans S., Sijtsma P., Mendez Lopez B. (2007), Location and quantification of noise sources on a wind turbine, *Journal of Sound and Vibration*, **299**(4–5): 869–883, doi: 10.1016/j.jsv.2006.07.032.

18. Ryi J., Choi J. (2017), Estimation method to achieve a noise reduction effect of airfoil with a serrated trailing edge for wind turbine rotor, *Noise Control Engineering Journal*, **65**(4): 345–355, doi: 10.3397/1/376550.